1. Send Roy Eason SH 3

E82-10394

# AgRISTARS

7 SR-P2-04278

5 NAS9-15466

NASA-CR-167644

A Joint Program for Agriculture and Resources Inventory Surveys Through Aerospace Remote Sensing



## Supporting Research

6 April 1982

Technical Report

# Soybean Canopy Reflectance as a Function of View and Illumination Geometry

3 by K. J. Ranson, V. C. Vanderbilt, L. L. Biehl, B. F. Robinson, and M. E. Bauer

(E82-10394) SOYBEAN CANOPY REFLECTANCE AS A FUNCTION OF VIEW AND ILLUMINATION GEOMETRY (Purdue Univ.) 16 p HC A02/MF A01 CSCL 02C N82-32816

Unclas

G3/43 00394

4 Purdue University
Laboratory for Applications of Remote Sensing
West Lafayette, Indiana 47907

SR-P2-04278
NAS9-15466
LARS 042182

# Soybean Canopy Reflectance as a Function of View and Illumination Geometry

K.J. Ranson, V.C. Vanderbilt, L.L. Biehl,
B.F. Robinson, and M.E. Bauer

Purdue University
Laboratory for Applications of Remote Sensing
West Lafayette, IN 47906

April 1982

## Star Information Form

**1. Report No.** SR-P2-04278

**2. Government Accession No.**

**3. Recipient's Catalog No.**

**4. Title and Subtitle**
Soybean Canopy Reflectance as a Function of View and Illumination Geometry

**5. Report Date** April 1982

**6. Performing Organization Code**


**7. Author(s)** K.J. Ranson, V.C. Vanderbilt, L.L. Biehl, B.F. Robinson, and M.E. Bauer


**8. Performing Organization Report No.** LARS 042182


**9. Performing Organization Name and Address**
Purdue University
Laboratory for Applications of Remote Sensing
1220 Potter Drive
West Lafayette, IN 47906-1399


**10. Work Unit No.**

**11. Contract or Grant No.** NAS9-15466


**12. Sponsoring Agency Name and Address**
NASA Johnson Space Center
Earth Resources Research Division
Houston, TX 77058


**13. Type of Report and Period Covered** Technical

**14. Sponsoring Agency Code**

**15. Supplementary Notes**


**16. Abstract**

In this paper we present the results of an experiment designed to characterize a soybean field by its reflectance at various view and illumination angles and by its physical and agronomic attributes. Reflectances were calculated from measurements at four wavelength bands through eight view azimuth and seven view zenith directions for various solar zenith and azimuth angles during portions of three days. An ancillary data set consisting of the agronomic and physical characteristics of the soybean field is described. These data sets should prove useful for validating most light interaction canopy models.

The results of the study indicate that the distribution of reflectance from a soybean field is a function of the solar illumination and viewing geometry, wavelength and row direction, as well as the state of development of the canopy. Shadows between rows greatly affected the reflectance in the visible wavelength bands and to a lesser extent in the near infrared wavelengths.

A model is proposed that describes the reflectance variation as a function of projected solar and projected viewing angles. The model appears to approximate the reflectance variations in the visible wavelength bands from a canopy with well-defined row structure.



**17. Key Words (Suggested by Author(s))**
Canopy Reflectance, Remote Sensing, Radiometer Data


**18. Distribution Statement**

**19. Security Classif. (of this report)** Unclassified

**20. Security Classif. (of this page)** Unclassified

**21. No. of Pages**

**22. Price**

# SOYBEAN CANOPY REFLECTANCE AS A FUNCTION OF VIEW AND ILLUMINATION GEOMETRY

K. J. Ranson, V. C. Vanderbilt, L. L. Biehl,
B. F. Robinson and M. E. Bauer

Purdue University
Laboratory for Applications of Remote Sensing
West Lafayette, Indiana 47907, U.S.A.

## ABSTRACT

In this paper we present the results of an experiment designed to characterize a soybean field by its reflectance at various view and illumination angles and by its physical and agronomic attributes. Reflectances were calculated from measurements at four wavelength bands through eight view azimuth and seven view zenith directions for various solar zenith and azimuth angles during portions of three days. An ancillary data set, consisting of the agronomic and physical characteristics of the soybean field is described. These data sets should prove useful for validating most light interaction canopy models.

The results of the study indicate that the distribution of reflectance from a soybean field is a function of the solar illumination and viewing geometry, wavelength and row direction as well as the state of development of the canopy. Shadows between rows greatly affected the reflectance in the visible wavelength bands and to a lesser extent in the near infrared wavelengths.

A model is proposed that describes the reflectance variation as a function of projected solar and projected viewing angles. The model appears to approximate the reflectance variations in the visible wavelength bands from a canopy with well defined row structure.

## 1. INTRODUCTION

The reflectance characteristics of an agricultural scene are a function of agronomic, geometric and atmospheric variables. Accurate characterization of agricultural crops from remotely measured spectral radiance or spectral reflectance is necessary if these data are to be used effectively for identification and condition assessment purposes.

In the past, researchers have noted that identification of agronomic variables from remote sensing data is affected by the dependence of canopy reflectance on the solar illumination and sensor viewing geometry. It is well known that increasing our understanding of this phenomenon will improve our abilities to monitor the physiological and phenological status of a crop.

*Presented at the Fifteenth International Symposium on Remote Sensing of Environment, Ann Arbor, MI, May 1981.

In recent years two goals have prompted researchers to measure the reflectance properties of crop canopies for various illumination and view conditions. First, the knowledge gained from analysis of empirical data, primarily acquired for nadir viewing conditions, has increased our understanding of spectral reflectance properties as they relate to the physiological and phenological status of a crop canopy. Daughtry et al, 1980, found relatively high correlations between spectral reflectance and such agronomic variables as biomass, percent ground cover, leaf area index and development stage of wheat. Leamer et al, 1980, showed that reflectance could be used to monitor crop development. A strong relationship between spectral radiance and grain yield of wheat was described by Tucket et al, 1980. Holben et al, 1980, found significant correlations between spectral radiance and soybean leaf area and biomass. All or the above studies utilized either truck-mounted or hand-held nadir viewing sensors. The need to extend this understanding to off-nadir viewing conditions is important due to the variations in view direction of airborne and satellite multispectral scanners and the selective pointing capabilities of future satellites such as the Systeme Probatoire d' Observation de la Terre (SPOT) (Chevrel et al, 1980) to be launched in this decade.

The second goal for acquiring reflectance data at off-nadir viewing angles is to provide data suitable for testing the accuracy of mathematical models which have been proposed to describe the radiance of a plant canopy for specific view and illumination conditions. An accurate model of the plant canopy reflectance could potentially provide the same information as is obtained from field observations, but without extensive field data acquisition activities. Analysis results of reflectance measurements have demonstrated that plant canopies are not simple Lambertian reflectors and thus not amenable to description by simple models (e.g., Suits, 1972; Smith and Oliver, 1974; Kimes et al, 1980; Vanderbilt, 1980). Since the models are not simple, their veracity must be tested vigorously, using data sets acquired under a variety of view/illumination and crop physiological and phenological conditions. As most canopy reflectance data have been acquired for nadir viewing conditions, only limited data acquired under a wide variety of view/illumination conditions are available for testing models. No extensive data set exists for soybeans, a crop of major economic importance.

In this paper we present the results of an experiment designed to characterize a soybean field by its reflectance at various view and illumination angles and by its physical and agronomic attributes. We discuss the reflectance differences obtained over a variety of view and illumination angles as affected by differences in the shadow between rows caused by the relationship between illumination, viewing and row directions. In addition, we propose a simple model to explain these reflectance variations. This model incorporates the concepts of projected solar angle and projected view angle to explain a portion of the reflectance variation due to shadows cast by rows.

## 2. MATERIALS AND METHODS

A commercial soybean field located approximately 16 km northeast of West Lafayette, Indiana was selected for this study. The field was planted to Calahan 9250 soybeans at a seeding rate of 62 kg/ha in north-south oriented rows planted 76 cm apart, resulting in about 28 plants/$m^2$. The field is in corn-soybean rotation and was hand-weeded prior to data acquisition to remove any volunteer corn and other weeds.

### Reflectance Measurements

The reflectance measurements were acquired on three clear days in the summer of 1980 (July 17, July 24 and August 28) with an Exotech model 100 radiometer with wavelength bands of .5-.6, .6-.7, .7-.8 and .8-1.1 μm. The field of view of the instrument was limited to 10° by a set of field stops attached to the viewing ports. The instrument was positioned on a truck-mounted aerial platform at a nominal elevation of 10 meters above the soil surface. The instrument was mounted on a panhead which allowed it to be positioned at specific view zenith and azimuth angles. The truck and associated instrument van and electrical generator were driven into the middle of the soybean field sufficiently distant from field edges to uniformly fill the field of view of the radiometer.

The measurement procedure consisted of positioning the boom of the aerial platform at an azimuth angle (from north) of 135° (Figure 1). At this position the instrument was set at a view zenith angle ($\theta_V$) of 7°. With $\theta_V$ held constant, spectral radiance measurements were made for view azimuth angles ($\theta_V$) of 0° (looking south), 315°, 270° (looking east), and 225°. This procedure was repeated for $\theta_V$ = 15°, 22°, 30°, 45° and 60°. The boom was rotated 180° and the process was repeated for $\phi_V$ = 180°, 135°, 90° and 45° with $\theta_V$ = 7°, 15°, 22°, 30°, 45° and 60°, thus completing a hemisphere of measurements. In addition to the off-nadir measurements, vertical canopy radiance was acquired at boom azimuth angles of 90°, 135°, 160°, 270°, 315° and 340°. In order to convert spectral canopy radiance to spectral reflectance factor (Robinson and Biehl, 1977), a 1.3 x 1.3 m calibration panel was viewed before and after each hemisphere measurement sequence. Just prior to the last calibration measurement, an area cleared of soybeans was measured with nadir view angle to provide data for bare soil spectral reflectance. Color photographs were taken with a boom-mounted 35mm camera coincident with each scene measurement. These photos were later used to identify any measurements where a boom shadow might influence the calculated reflectance.

This procedure was repeated at roughly one-half hour intervals as long as cloud conditions remained satisfactory (Table 1). Care was taken to avoid taking measurements when the sun was obscured or when individual cumulus type clouds were within 15° of the solar disk.

Meteorological data consisting of relative humidity, air temperature, barometric pressure, wind direction, wind speed and global solar irradiance were measured on each day at the Purdue Agronomy Farm located about 6 km southeast of the study site. As an indication of the irradiance variation at the site, an upward-looking photocell was monitored throughout the measurement periods. In addition, shaded calibration panel measurements were taken on each of the three days to estimate the proportion of skylight present.

Agronomic Measurements

Agronomic and physical characteristics of the soybean field were measured the day after each reflectance data acquisition date. The agronomic measurements consisted of sampling fresh and dry biomass, leaf area index, average canopy height and width and development stage. Physical measurements included leaf inclination angle, leaf azimuth angle, leaf area and three-dimensional leaf position. In addition, individual leaf reflectance and transmission measurements were obtained using live plants.

Soybean biomass was estimated by harvesting plants in 1.0 m lengths of row at randomly located positions within the field. Each sample was placed in plastic bags and weighed to determine fresh biomass. The soybeans were then separated into green leaflets, yellow leaves, stems plus petioles and pods, dried at 60° C and reweighed. A random subsample of green leaf area from each sample was measured with an optical device (Lambda Instrument Co. Model I-3000) and the ratio of leaf area to leaf dry weight was estimated. Leaf area index was calculated using this leaf area: Leaf weight ratio and the total dry weight of green leaflets from plans in a 1.0 m length of row. Development stage was estimated based on the Fehr and Caviness scale (Fehr and Caviness, 1977). In addition, estimates of percent ground cover were made from the vertical color photographs obrained during reflectance data acquisition.

Physical Measurements

Three-dimensional characterization of the soybean canopy was accomplished by measuring leaflet heights, distances from mid-row and distances along row as references to a 1 m x 1.3 m board with a grid of meter sticks attached to it. Leaflet inclination angles were determined with an inclinometer similar to those described by Nichiporovich (1961) and Kyle and Davies (1974). Azimuths were measured with a simple apparatus consisting of a small plate equipped with a circular bubble level and a dowel attached perpendicular to the face of the plate.

The location of the sample was randomly determined by throwing a meter stick out into the field. The measurement board was then placed in this location in the furrow halfway between adjacent rows and a windbreak was constructed to protect the sample from wind. The board was then leveled and positioned vertically. The distance between the bottom of the board and the base of the plants was measured to correctly determine the leaflet heights. All leaflets within a 25 cm length of row were sampled starting with the uppermost leaf and progressing downward. Leaflet azimuth angles were measured by orienting the bubble level plate towards true north and then placing it parallel to the upper leaflet surface. The bubble level was graduated into 45° segments with the position of the bubble indicating the azimuth + 180°. With the azimuth device still in place, the inclinometer was held parallel to the perpendicular dowel on the plate, thus indicating the angle from vertical to the leaf normal. The recorded angle was later converted to inclination. After the angle measurements were made, a meter stick was placed above the leaf and the distance from the center of the leaflet to the measurement board was recorded. Being sure the meter stick was perpendicular with the measurement board, we recorded the distance from a reference point on the board to the center of the leaflet and the height of the leaflet. The leaflet was then removed from the plant, numbered with a felt marking pen and placed in an ice chest for later leaf measurement. Individual leaf areas were determined with an optical leaf area meter later the same day in the laboratory.

The geometry estimation procedure was performed simultaneously by two teams at different locations in the field. Each crew, consisting of a measurement person and a recorder, received over 4 hours training prior to the first data collection period. All destructive sampling was conducted outside the total field of view perimenter for the reflectance measurements.

3. RESULTS

The estimates of the agronomic variables for the three days are summarized in Table 2. The soybean canopy developed rapidly between the first and second measurement dates with ground cover increasing from 72% to 83%, indicating that the canopy was increasing in density and rapidly losing its previously well defined row structure. By the last measurement date, the canopy was completely overlapping with a ground cover of 99%; however, LAI had decreased about 10%.

The distribution of leaf inclination angles changed rapidly from a more or less planophile type (mostly horizontal leaves) on the first date to having a greater proportion of vertically inclined leaves on the second and third dates. Blad and Baker (1972) reported that soybean leaves distribution tends to be more planophile through most of the growing season, with leaves distributed almost evenly in the early and late growth stages. We suspect that the departure of the leaf distribution on the second day from a planophile type to a more evenly distributed arrangement is due to wilting caused by the very high temperatures and lack of rainfall prior to and during this date. Figure 2 presents the leaf angle distributions weighted by leaf area for the three dates.

To evaluate how the changes discussed above affect the reflectance from the soybean field, reflectance factors for each of the four wavelength bands were plotted over solar zenith angle, $\theta_s$ for a nadir sensor viewing angle ($\theta_v$ = 0°) (Figure 5). The soybean canopy reflectance factor ($R_C$) increased slightly with increasing $\theta_s$ for the two near infrared wavelength bands. Quite a different trend was observed for the two visible bands for the first two dates. $R_C$ was the largest in both bands when the sun was at its highest position in the sky, then decreased to a point and then leveled off through steeper $\theta_s$. This trend was reported by Kollenkark et al, 1981, to be mainly the effect of changing shadows cast between rows of soybeans. The point at which the reflectance begins leveling off is a function of $\theta_s, \varphi_s$ and the canopy geometry. Where canopy geometry is described in terms of the across-row canopy profile (Figure 3), it can be shown that a critical solar angle ($\theta_c$) defines the point where soil between the rows seen by a nadir looking sensor becomes completely shaded. Thus at $\theta_s < \theta_c$ sunlit bare soil is present in the scene.

The reflectance factors in the visible band for the third measurement date when the canopy was overlapping follows the same trend as the near IR reflectances. This suggests that completely developed canopies are affected to a lesser extent by changes in $\theta_s$ than canopies with well defined row structure. This isn't meant to imply that overlapping soybeans approximate a Lambertian surface; rather, quite the opposite is true, as we will discuss later.

The reflectance of bare soil decreased gradually as $\theta_s$ increased for all four wavelength bands for all three dates (Figure 5). This gradual decrease was not due to shadows cast by soybean rows, but was more likely due to surface roughness effects caused by soil clods and furrows.

It is apparent from the above results that the reflectance in the two visible wavelength bands of a soybean field is strongly affected by shadows cast by rows. This effect is not as strong in the near infrared bands nor is it apparent in the visible bands for an overlapping canopy.

Analysis of the reflectance factors for varying view and illumination geometry shows quite dramatically the non-Lambertian character of the soybean field. Figure 6 presents polar graphs of equal reflectance contours for the .6-.7 μm and .8-1.1 μm wavelength bands over a hemisphere of viewing zenith and azimuth angles at two different times for each date. To interpret these graphs, the reader is referred to Figure 4 which describes the positions of the view zenith and azimuth angles of the measurement hemispheres.

For the July 17 measurements, graphs are presented for hemispheres of reflectance factors acquired at midday and late afternoon (Table 1). In the first hemisphere, the distribution of reflectance factors for the visible band can be likened to a hill elongated along the row direction ($\phi_r$). Reflectance falls off more rapidly at $\phi_v = \phi_r \pm 90°$ than it does at $\phi_v = \phi_r \pm 180°$. The near infrared reflectance, however, is maximum in the direction toward the sun and decreases to a minimum away from the sun at $\theta_v = 30°$, and then increases slightly in the same direction for steeper $\theta_v$. For the second hemisphere where $\theta_s$ is at nearly right angles with $\phi_r$, the reflectance factors approximate a bowl with a steep side towards the sun. A similar pattern occurs with the near infrared band reflectances.

For July 24, hemispheres are presented for midmorning and midday. The visible reflectance distribution for the first hemisphere shows a somewhat similar pattern to that of the first July 17 hemisphere with a maximum occurring near $\theta_v = 20°$, $\phi_v = 0°$. The near infrared reflectance is highest at $\theta_v = 30°$ in the direction towards the sun and decreases away from the sun. The second hemisphere has maximum visible band reflectance at $\theta_v = 40°$ in the direction of the sun and a minimum at $\theta_v = 20°$ away from the sun. The near infrared reflectance is also maximized towards the sun at $\theta_v = 50°$ and decreases away from the sun. The August 27 hemispheres acquired at midday and late afternoon all show bowl -like distribution with the steepest side toward the direction of the sun for both wavelength bands.

ORIGINAL PAGE IS
OF POOR QUALITY

It appears that the reflectance distribution of the soybean field has a maximum where the viewing and illumination angles coincide near the hot spot. We can infer this only indirectly since when spectral data were acquired at the hot spot, the field of view contained the shadow of the instrument and these data were not included in this analysis.

In the .6-.7 μm wavelength, region shadows between rows are the dominant feature in the scene. The amount of shadows is a function of the canopy geometry and the position of the sun relative to the row. Reflectance measurements from a vertical-looking sensor are a function of the changing shadows as the solar zenith angle changes. As the view angle changes, more or less shaded soil and canopy are viewed, thus either decreasing or increasing the reflectance.

If the sun azimuth is in line with the row direction, then the amount of shaded soil will be minimized. With the view azimuth also equal to the row direction, the canopy reflectance will be maximized at the hot spot. If the view azimuth direction is at right angles to the sun and row direction, reflectance will decrease as the view zenith angle increases due to less sunlit soil and more canopy shadows being present.

If the sun's azimuth is at right angles to row direction, then reflectance will be maximized at the hot spot and will decrease at smaller view angles due to shaded soil. If the view azimuth is 180° from the sun, reflectance increases with view angle, possibly due to forward-scattered light.

We can describe the relationship of viewing and illumination angles with row direction as projected view angle($\theta_{vp}$) and projected solar angle ($\theta_{sp}$), as discussed by Verhoef and Bunnik, 1976, and Kollenkark et al, 1981. That is, $\theta_{sp} = \mathrm{TAN}^{-1}(\tan\theta_s \sin(\phi_s - \phi_r))$ and $\theta_{vp} = \mathrm{TAN}^{-1}(\tan\theta_v \sin(\phi_v - \phi_r))$. Additionally, we can describe a critical angle ($\theta_c$) as that $\theta_{sp}$ where the soil is completely shaded.

Let us first assume a square-shaped canopy where only sunlit foliage and sunlit soil contribute to the canopy radiance (i.e., shaded foliage and soil are black) and the sunlit portion of the canopy approximates a Lambertian surface. Then we can describe a model that should account for varying reflectance as a function of view and illumination geometry. We identify limits of $\theta_{sp}$, $\theta_{vp}$ and $\theta_c$ where the reflectance should have nearly equal reflectance. When $90° \geq \theta_{sp} \geq \theta_c$ and $90° > \theta_{vp} \geq \theta_{sp}$, then we have the case of the canopy hot spot. In this region only radiance from the sunlit top of the canopy impinges the sensor and $R(\theta_{sp}, \theta_{vp})$ will approximate $R(\theta_{sp}, \theta_{sp})$. For the case where $90° \geq \theta_{sp} \geq \theta_c$ and $0° < \theta_{vp} < \theta_{sp}$, the sensor sees proportionately more shadow so $R(\theta_{sp}, \theta_{vp})$ will be less than the hot spot reflectance and equal to the case where $0° \leq \theta_{sp} \leq \theta_c$ and $0° < \theta_{vp} < \theta_{sp}$. Assigning a negative sign to view directions from the left side of the row and making the additional assumption that the canopy is symmetrical along the row, then when $90° \geq \theta_{sp} > \theta_c$ and $-90° < \theta_{vp} < 0°$ or $0° \leq \theta_{sp} \leq \theta_c$ and $-90° < \theta_{vp} < 0°$, then $R(\theta_{sp}, \theta_{vp})$ will be about equal to the reflectance for a given $\theta_{sp}$ and a nadir-looking sensor. If we have $0° \leq \theta_{sp} \leq \theta_c$ and $\theta_c > \theta_{vp} \geq \theta_{sp}$, then if the canopy is viewed from $\theta_c$, the reflectance will be least when $\theta_{vp} = \theta_c$ and will increase up to the hot spot position. Finally, when $0° \leq \theta_{sp} \leq \theta_c$ and $0° < \theta_{vp} < \theta_{sp}$, then the sensor will see the same amount of shaded soil and canopy and the reflectance will approximate $R(\theta_{sp}, \theta_c)$. A summary of these results is presented in Table 3.

Areas of equal reflectance can be identified on the basis of the difference between $\theta_{sp}$ and $\theta_{vp}$, as shown in Figure 7. Analysis of our reflectance data in the .6-.7 μm band indicates this model is a reasonable first approximation to the complex distributions of reflectance obtained over a wide range of view and illumination angles. It is, however, quite apparent that it fails to deal with the multiple scattering, both diffuse and specular, that complicates the reflectance distribution in both the visible and near-infrared bands.

## 4. SUMMARY

The rather complex distribution of reflectance from a soybean field over varying view/illuminaton conditions has been discussed. It is evident that the reflectance distribution is a function of the solar and viewing geometry, wavelength, and row direction as well as the state of development of the canopy. Shadows between rows greatly affected the reflectance from the field in the visible wavelength bands and to a much lesser extent the near-infrared band reflectances.

The results of the experiments discussed should provide a data set suitable for testing various canopy models that predict the reflectance as a function of view and illumination conditions, canopy geometry and agronomic variables. A document further describing this data set will be forthcoming later this year.

A model was proposed that describes the expected variation of reflectance in terms of the difference between projected solar and projected view angles. The assumptions of the model limits its applicability to row canopies and the highly absorptive red wavelength band. It does, however, provide an initial framework for understanding the rather complex reflectance variations of a soybean canopy as a function of view and illumination conditions.

## 5. ACKNOWLEDGEMENTS

The authors wish to thank Mr. Joe Kerkhove, the owner of the soybean field, for his cooperation in this study. In addition, we wish to cite the LARS personnel who assisted in the field data collection, Lou Nash, Diana Braddick, Carol McFadyen and Donna Parker.

The research was sponsored by the NASA Johnson Space Center under Contract No. NAS9-15466.

## 6. REFERENCES

Blad, B.L. and D.G. Baker. 1972. Orientation and distribution of leaves within a soybean canopy. Agron. J. 4:26-29.

Daughtry, C.S.T., M.E. Bauer, D.W. Crecelius and M.M. Hixson. 1980. Effects of management practices on reflectance of spring wheat canopies. Agron J. 72(6):1055-1060.

Chevrel, M., M. Courtois and G. Weill. 1980. The SPOT satellite remote sensing mission. Proc. 1980 ACSM-ASP Convention, St. Louis, MO.

Fehr, W.R. and C.E. Caviness. 1977. Stages of soybean development. Special report 80. Cooperative Extension Service, Iowa State University of Science and Technology, Ames, IA, 12 pp.

Holben, B.N., C.J. Tucker and C. Fan. 1980. Spectral assessment of soybean leaf area and leaf biomass. Photogramm. Eng. and Remote Sensing 46(5):651-656.

Kimes, D.S., J.A. Smith and K.J. Ranson. 1980. Vegetation reflectance measurements as a function of solar zenith angle. Photogramm. Eng. and Remote Sensing 46(12):1563-1573.

Kollenkark, J.C., V.C. Vanderbilt, C.S.T. Daughtry and M.E. Bauer. 1981. Canopy reflectance as influenced by solar illumination angle. AgRISTARS Technical Report SR-PO-04039. LARS Technical Report 021681. Laboratory for Applications of Remote Sensing, Purdue University, W. Lafayette, IN 47907. 20 pp.

Kyle, W.J. and J.A. Davies. 1974. Quantitative comparison of foliage display in two plots of corn. Can. J. Bot. 52:2465-2471.

Leamer, R.W., J.R. Noriega and A.H. Gerberman. 1980. Reflectance of wheat cultivars as related to physiological growth stages. Agron. J. 72(6):1029-1032.

Nichiporovich, A.A. 1961. Properties of plant crops as an optical system. Sov. Plant Physiol. 8:428-435.

Robinson, B.F. and L.L. Biehl. 1979. Calibration procedures for measurement of reflectance factor in remote sensing field research. Proc. Soc. Photo-Optical Instrumentation Engr. 23rd Annual Tech. Symp. on Measurements of Optical Radiation, Bellingham, WV, pp 16-26.

Smith, J.A. and R.E. Oliver. 1974. Effects of changing canopy directional reflectance on feature selection. Applied Optics 13(7):1599-1604.

Suits, G.H. 1972. The calculation of the directional reflectance of a vegetative canopy. Remote Sens. Environ. 2:117-125.

Tucker, C.J., B.N. Holben, J.H. Elgin and J.E. McMurtry III. 1980. Relationship of spectral data grain yield variation. Photogramm. Eng. Remote Sensing. 46(5):657-666.

Vanderbilt, V.C., B.F. Robinson, L.L. Biehl, M.E. Bauer and A.S. Vanderbilt. 1980. Simulated response of a multispectral scanner over wheat as a function of wavelength and view/illumination directions. ISP Congress, Hamburg, W. Germany.

Verhoef, W. and N.J.J. Bunnik. 1976. The spectral directional reflectance of row crops. NIWARS, No. 35. 3 Kanaalweg, left, The Netherlands. 134 pp.

ORIGINAL PAGE IS
OF POOR QUALITY

Table 1. Illumination Conditions for Spectral Data Collection

| Solar Angle Period | Time Period Start (GMT) | Time Period Stop (GMT) | Solar Zenith Angle Range Max. - Min. - Max. (Degrees) | Solar Azimuth Angle Range (Degrees) | Cloud Cover % |
|---|---|---|---|---|---|
| Date: July 17, Day of Year: 199 | | | | | |
| 1* | 17:59 | 18:32 | 19 - 21 | 183-205 | 10 |
| 2 | 19:03 | 19:29 | 24 - 28 | 222-233 | 10 |
| 3 | 19:47 | 20:06 | 31 - 34 | 240-245 | 20 |
| 4 | 20:28 | 20:49 | 38 - 42 | 251-256 | 10 |
| 5* | 21:19 | 21:35 | 47 - 50 | 262-265 | 10 |
| Date: July 18, Day of Year: 206 | | | | | |
| 1* | 15:14 | 15:31 | 40 - 37 | 109-113 | 1 |
| 2 | 15:51 | 16:06 | 33 - 31 | 119-124 | 20 |
| 3 | 16:31 | 16:51 | 27 - 25 | 133-142 | 10 |
| 4 | 17:10 | 17:25 | 23 - 22 | 152-161 | 5 |
| 5* | 17:51 | 18:06 | 21 | 178-188 | 5 |
| 6 | 18:36 | 18:49 | 22 - 24 | 206-214 | 20 |
| Date: August 27, Day of Year: 240 | | | | | |
| 1 | 15:55 | 16:14 | 40 - 37 | 132-139 | 0 |
| 2 | 16:23 | 16:39 | 36 - 34 | 142-148 | 0 |
| 3 | 17:07 | 17:23 | 32 - 31 | 160-167 | 0 |
| 4 | 17:30 | 17:45 | 31 - 30 | 171-178 | 0 |
| 5* | 18:17 | 18:31 | 31 - 32 | 193-200 | 0 |
| 6 | 18:38 | 18:52 | 32 - 33 | 203-209 | 0 |
| 7 | 19:06 | 19:20 | 35 - 36 | 214-220 | 0 |
| 8 | 19:27 | 19:43 | 37 - 39 | 222-227 | 0 |
| 9 | 20:10 | 20:23 | 43 - 46 | 235-239 | 0 |
| 10 | 20:32 | 20:46 | 47 - 49 | 241-245 | 0 |
| 11* | 21:08 | 21:26 | 53 - 56 | 249-253 | 0 |
| 12 | 21:42 | 21:59 | 59 - 60 | 256-237 | 0 |

* Indicates measurement hemispheres shown in Figure 6.

Table 2. Agronomic Measurements

| Date | Leaf Area Index | Total Fresh Biomass $g/m^2$ | Total Dry Biomass $g/m^2$ | Ground Cover % | Height cm | Width cm | Maturity Stage |
|---|---|---|---|---|---|---|---|
| July 18 | 3.0 | 1145 | 230 | 72 | 69 | 58 | V13R3 |
| July 25 | 3.9 | 1540 | 320 | 83 | 84 | 69 | V14R3 |
| Aug. 28 | 2.8 | 2535 | 645 | 99 | 102 | 104 | V20R6 |

ORIGINAL PAGE IS
OF POOR QUALITY

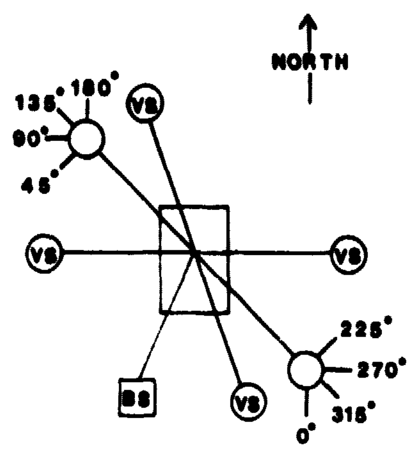


Figure 1. Diagram of boom positions for measurement of reflectance hemispheres. VS = vertically viewed soybeans. BS = vertically viewed bare soil.

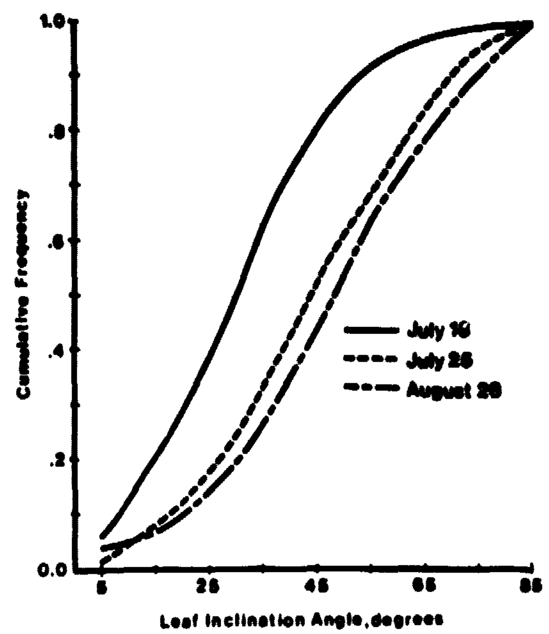


Figure 2. Cumulative leaf angle inclination distribution weighted by leaf area.

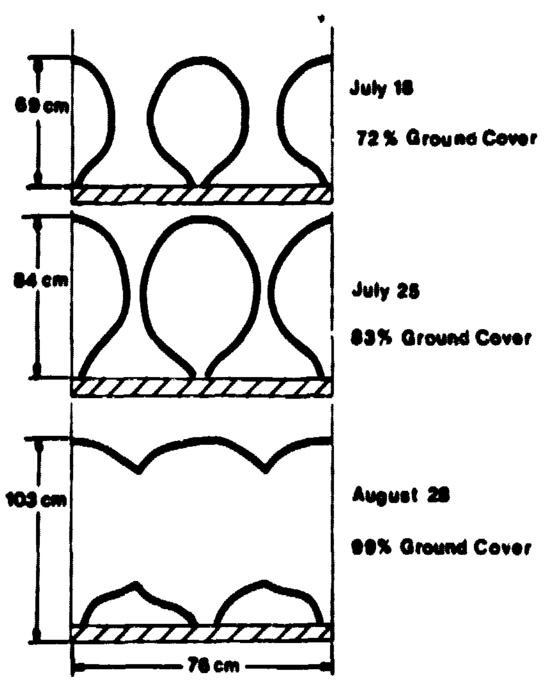


Figure 3. Idealized canopy profiles for three measurement dates.

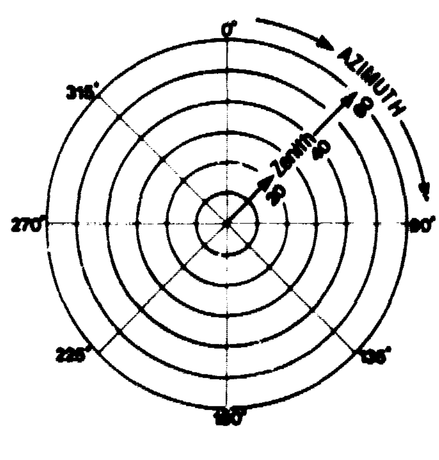


Figure 4. Diagram of view zenith and azimuth angles used for contour plots of equal reflectance shown in Figure 6.

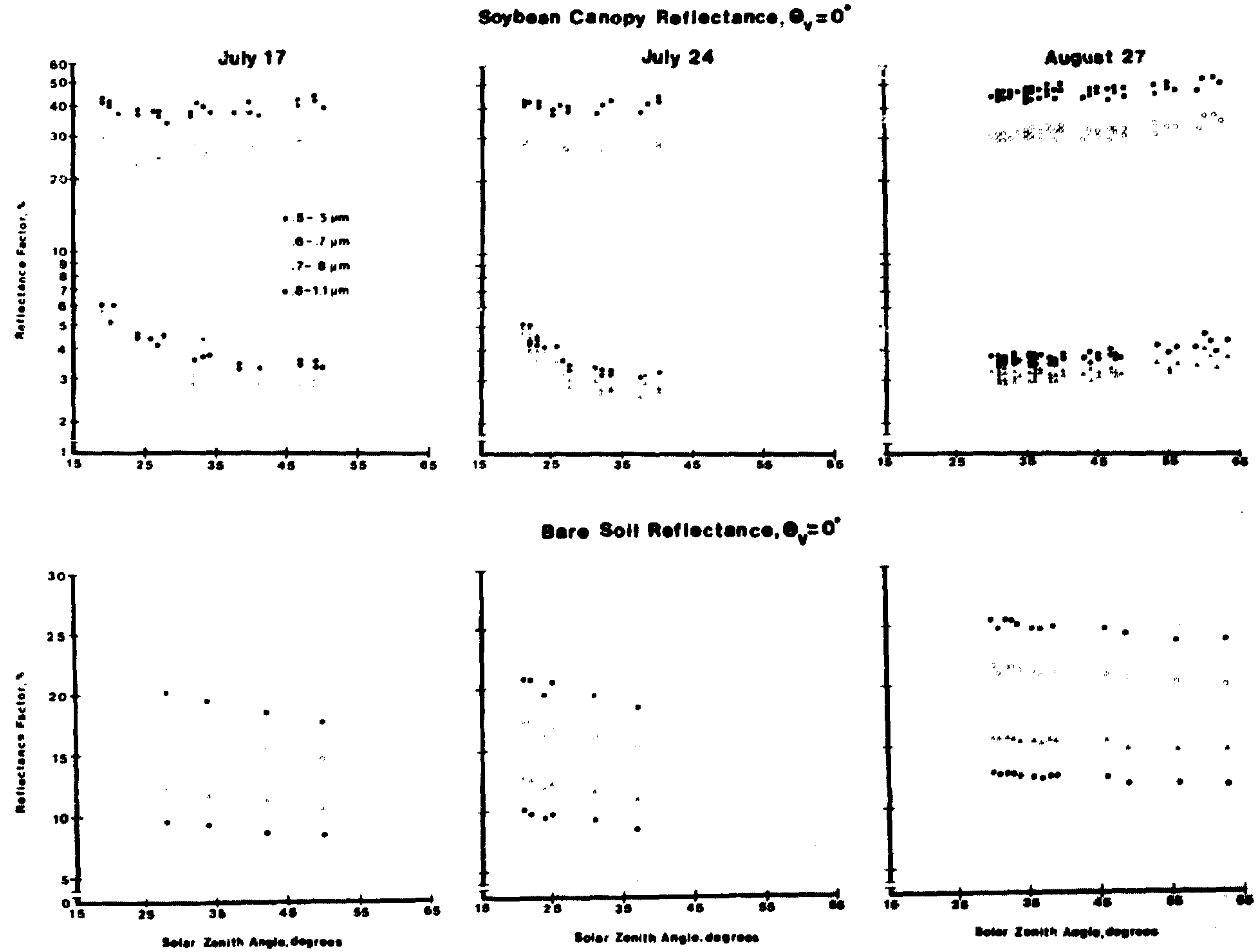


Figure 5. Relationships of soybean canopy and bare soil reflectance factors and solar zenith angle on three days for a nadir looking sensor.

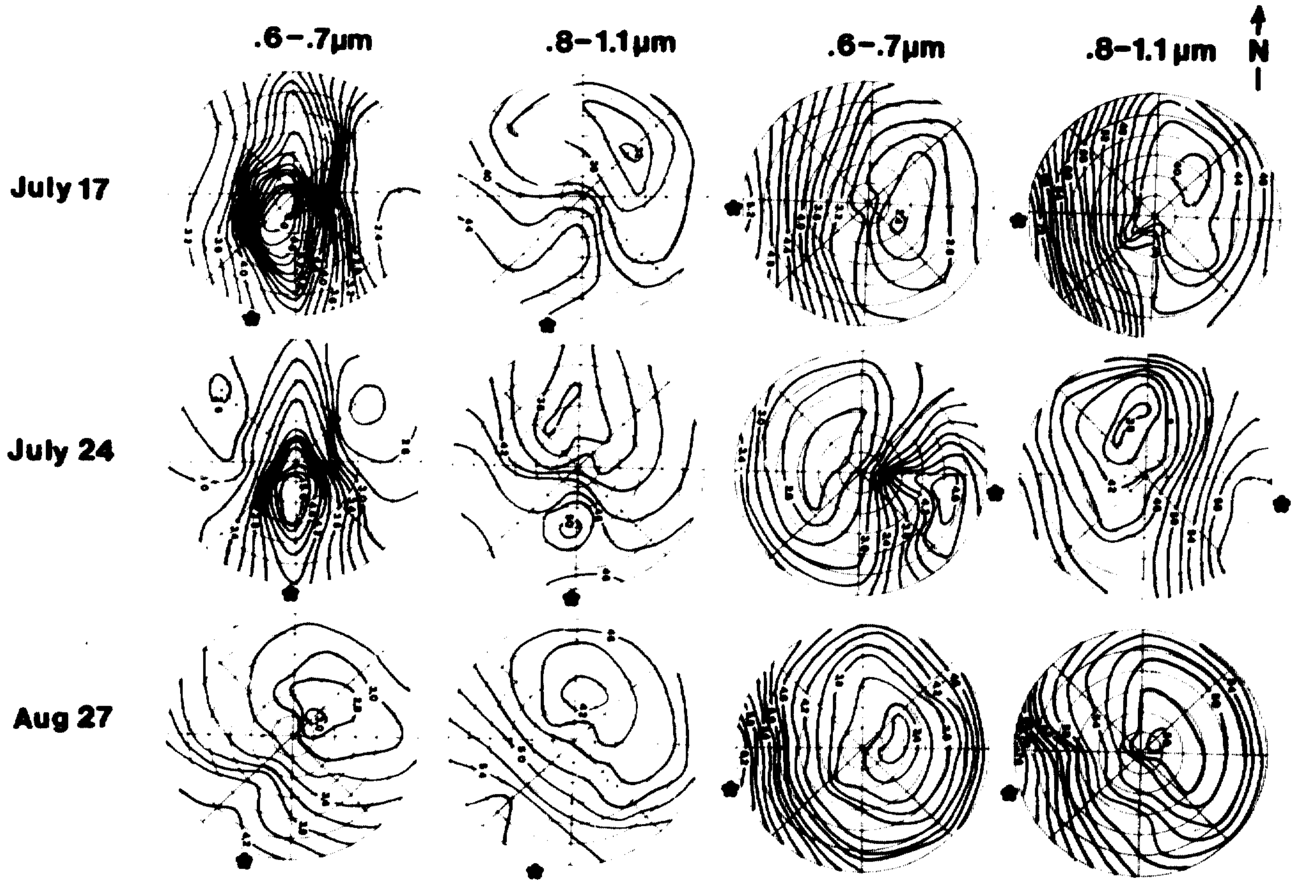


Figure 6. Contours of equal reflectance for three dates, two wavelength bands and two measurement hemispheres. Solid stars indicate solar azimuth position.

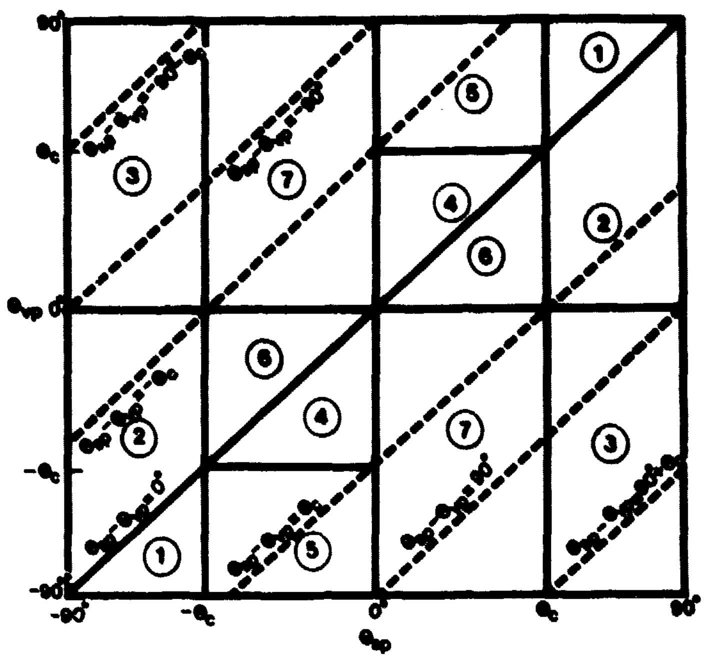


Figure 7. Model diagram of $\theta_{sp}$, $\theta_{vp}$ plane. Numbered regions within solid lines indicate areas of nearly constant reflectance defined by $\theta_{sp}$, $\theta_{vp}$ and $\theta_c$ (see Table 3). Dashed lines represent equal values of $\theta_{sp} - \theta_{vp}$ angles.

Table 3. Summary of Reflectance Relationships for Angular Limits of $\theta_{sp}$, $\theta_{vp}$ and $\theta_c$.

| Area of $\theta_{sp}$,$\theta_{vp}$ Plane | Angle Limits | Reflectance |
|---|---|---|
| 1 | $90° \geq \theta_{sp} \geq \theta_c$, $90° \geq \theta_{vp} \geq \theta_{sp}$ | $R(\theta_{sp},\theta_{vp}) \approx R(\theta_{sp},\theta_{sp}) \approx$ constant |
| 2 | $90° \geq \theta_{sp} \geq \theta_c$, $0 < \theta_{vp} < \theta_{sp}$ | $R(\theta_{sp},\theta_{vp}) < R(\theta_{sp},\theta_{sp})$ |
| 3 | $90° \geq \theta_{sp} \geq \theta_c$, $-90° < \theta_{vp} < 0°$ | $R(\theta_{sp},\theta_{vp}) \approx$ constant $\approx R(\theta_{sp},0)$ |
| 4 | $0° \leq \theta_{sp} \leq \theta_c$, $\theta_c \geq \theta_{vp} \geq \theta_{sp}$ | $R(\theta_{sp},\theta_c) < R(\theta_{sp},\theta_{vp}) < R(\theta_{sp},\theta_{sp})$ |
| 5 | $0° \leq \theta_{sp} \leq \theta_c$, $90° \geq \theta_{vp} \geq \theta_c$ | $R(\theta_{sp},\theta_{vp}) \approx R(\theta_{sp},\theta_c) \approx$ constant |
| 6 | $0° \leq \theta_{sp} \leq \theta_c$, $0° < \theta_{vp} < \theta_{sp}$ | $R(\theta_{sp},\theta_{vp}) < R(\theta_{sp},\theta_{sp})$ |
| 7 | $0° \leq \theta_{sp} \leq \theta_c$, $-90° < \theta_{vp} < 0°$ | $R(\theta_{sp},\theta_{vp}) \approx R(\theta_{sp},0) \approx$ constant |